Eckhaus Instability in Systems with Large Delay

Matthias Wolfrum[1,*] and Serhiy Yanchuk[1,2,3,†]

[1]Weierstrass Institute for Applied Analysis and Stochastics, Mohrenstrasse 39, D-10117 Berlin, Germany
[2]Institute of Mathematics, Humboldt-University of Berlin, Unter den Linden 6, D-10099 Berlin, Germany
[3]Institute of Mathematics, National Academy of Sciences of Ukraine, Tereshchenkivska 3, 01060 Kiev, Ukraine

(Received 17 February 2006; published 9 June 2006)

The dynamical behavior of various physical and biological systems under the influence of delayed feedback or coupling can be modeled by including terms with delayed arguments in the equations of motion. In particular, the case of long delay may lead to complicated and high-dimensional dynamics. We investigate the effects of delay in systems that display an oscillatory instability (Hopf bifurcation) in the absence of delay. We show by analytical and numerical methods that the dynamical scenario includes the coexistence of multiple stable periodic solutions and can be described in terms of the Eckhaus instability, which is well known in the context of spatially extended systems.

DOI: 10.1103/PhysRevLett.96.220201 PACS numbers: 02.30.Ks, 02.30.Oz, 05.45.−a

Differential equations with delayed argument $\dot{y} = \mathcal{F}(y, y_\tau)$, where $y_\tau = y(t - \tau)$, turned out to be a useful tool for studying many physical and biological systems. Already in scalar equations the effect of the delay can lead to complicated dynamics, and there are extensive studies for a large variety of scalar equations describing, e.g., population dynamics [1], physiological control systems [2], or delayed phase-locked loops [3,4]. In particular, it has been shown that the dynamics can become high-dimensional if the delay is large [3,5].

In the case of scalar equations, the dynamics without delay are always trivial and all complicated effects are induced by the delay. In systems of two or more variables, one can observe nontrivial dynamics already without delay, and it is an important question how these dynamics are affected by introducing delayed terms.

Here we will investigate the interplay of an oscillatory instability (Hopf bifurcation) with a long delayed feedback. As a paradigm for this very general situation, we choose the equation

$$z' = (\alpha + i\beta)z - z|z|^2 + z_\tau, \tag{1}$$

where $z(t)$ is a complex variable and α, β are real parameters. Neglecting the feedback term, this system is just the normal form for a supercritical Hopf bifurcation, in which for increasing α at $\alpha = 0$ the trivial solution $z \equiv 0$ becomes unstable, and a stable periodic solution with frequency β bifurcates. In the presence of the delay term, this simple destabilization scenario changes drastically. It appears to be twofold: Already for $\alpha = -1$ the trivial solution becomes weakly unstable, and, in a scenario similar to the Eckhaus instability in spatially extended systems, a large number of coexisting periodic attractors appears. With further increasing bifurcation parameter α, the stationary state becomes strongly unstable and the system exhibits an instability to a single periodic attractor. The bifurcation parameter mediates the transition between these two states, one of which is essentially multidimensional and the other is low-dimensional.

Examples of systems where this scenario can be found are lasers with delayed feedback [6,7], ecological systems with multiple species and delay [1], neural networks [8], damped oscillators with delayed forcing [9], etc. Another particular example is the method of time-delayed-feedback control [10]. We want to emphasize that Eq. (1) should be considered as a generic model, describing the behavior of any system with large delay and certain spectral conditions, which will be specified below.

The plan of our Letter is as follows: First, we perform a linear stability analysis of the stationary state in order to identify parameter values where it is weakly or strongly unstable. This gives us the distinction between the two stages in the destabilization scenario. Then we show numerically that close to the initial destabilization at $\alpha = -1$ multiple coexisting periodic attractors occur. We show that this scenario can be described by the Eckhaus phenomenon, which is one the basic mechanisms of pattern formation in spatially extended systems [11–16]. To this end, we derive a complex Ginzburg-Landau (GL) equation with specific boundary conditions as an amplitude equation which can describe the behavior of solutions in a vicinity of the destabilization threshold. The existence of Eckhaus instability in the amplitude equation then implies a similar behavior in the delay system in this stage. We also note that the above mentioned spatiotemporal representation fails with further increasing of the bifurcation parameter.

Stability analysis.—We start with an analytical stability analysis of the stationary state $z = 0$ and identify the parameter values leading to either weak or strong instability. The growth rate λ of small perturbations $e^{\lambda t}$ is determined by solutions of the characteristic equation

$$\lambda - (\alpha + i\beta) - e^{-\lambda\tau} = 0. \tag{2}$$

Equation (2) has infinitely many solutions, which can be expressed, for instance, via the complex Lambert function

[10]. Since we consider the case of large delay τ, we are interested in the asymptotics of these roots as $\tau \to \infty$. Therefore, it is convenient to introduce a small parameter $\varepsilon = 1/\tau$. As shown in Refs. [17,18] for more general cases, the characteristic Eq. (2) has two types of solutions, which have different asymptotical properties with respect to ε: (i) strongly unstable eigenvalues $\lambda_S = \alpha + i\beta + \mathcal{O}(\varepsilon)$ for $\alpha > 0$, which originate from the instantaneous terms; (ii) pseudocontinuous spectrum of eigenvalues, which, up to the leading order in ε, can be approximated as $\lambda_P(\omega) = i\omega + \varepsilon\gamma(\omega)$. Here the parameter ω admits a countable set of values $\omega = \omega_k = \omega_0 + 2\pi k\varepsilon$, $k = 0, \pm 1, \pm 2, \ldots$. By substituting λ_P into (2), we obtain in leading order

$$\gamma(\omega) = -\tfrac{1}{2}\ln[\alpha^2 + (\omega - \beta)^2]. \qquad (3)$$

The function $\gamma(\omega)$ is the rescaled real part of λ_P and determines the stability of the stationary state for $\alpha < 0$. Recall that for $\alpha > 0$ a strongly unstable eigenvalue appears. The pseudocontinuous spectrum is illustrated in Fig. 1(a). One can see the curves $[\mathrm{Re}\lambda/\varepsilon = \gamma(\omega), \mathrm{Im}\lambda = \omega]$, along which the eigenvalues are located at discrete positions, corresponding to $\omega = \omega_k$ with small distances $2\pi\varepsilon$ between each other. These curves persist as delay is increased and are filled more and more densely with eigenvalues.

One can see that the pseudocontinuous spectrum implies instability for $|\alpha| < 1$. At $|\alpha| = 1$, the curve touches the imaginary axis at the critical frequency β. Hence, in contrast to the Hopf bifurcation in the system without delay, the loss of stability happens already for $\alpha = -1$. With increasing control parameter α, the stationary state becomes unstable to perturbations of the form $e^{i\omega t}$, where ω belongs to some interval around β. These unstable frequencies can be obtained from (3) by the condition $\gamma(\omega) > 0$, i.e., $\alpha^2 + (\omega - \beta)^2 < 1$. Figure 1(b) illustrates these frequencies and summarizes the main conclusions of the stability analysis: (i) For $\alpha < -1$, the stationary state is stable; (ii) for $-1 < \alpha < 0$, it is weakly unstable; i.e., it has unstable eigenvalues from the pseudocontinuous spectrum with real parts proportional to ε; (iii) for $\alpha > 0$, it is strongly unstable, possessing the eigenvalue $\lambda_S \approx \alpha + i\beta$.

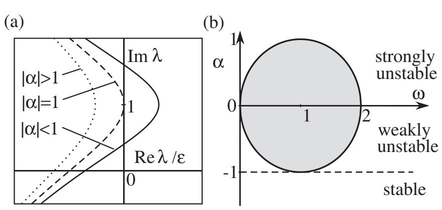

FIG. 1. Linear stability of system (1). (a) Curves of pseudocontinuous spectrum, along which eigenvalues accumulate for large delay, shown for three different parameter values. Solid line: $\alpha = 0.8$; dashed line: $\alpha = 1$; dotted line: $\alpha = 1.2$. Destabilization occurs at $|\alpha| = 1$. (b) The interval of unstable frequencies ω is shown in gray for different values of parameter α. These frequencies correspond to the interval of $\mathrm{Im}\lambda$, for which the pseudocontinuous spectrum from (a) is unstable (weak instability). In addition, the strong instability region for $\alpha > 0$ is indicated. $\beta = 1$ is fixed.

Note that strongly unstable eigenvalues from the instantaneous part and weakly unstable pseudocontinuous spectrum can be calculated similarly in any system with large delay. In this way, the spectral conditions for appearance of the Eckhaus scenario can be verified easily in any specific model equation.

Numerical results.—In our numerical simulations, we fix $\beta = 1$. First, we choose the bifurcation parameter $\alpha = -0.8$, such that the stationary state is already weakly unstable. The results of the integration for system (1) are shown in Fig. 2. For convenience, we show the orbit of the delay system using a "spatiotemporal" representation [19]. Roughly speaking, the horizontal axis corresponds to the spacelike coordinate ranging from 0 to τ and the vertical axis to some rescaled slow time t/τ^3. The precise meaning of the axes will become clear below, when the amplitude equations are introduced. Such a representation is useful, since it shows the solution over a time interval of order τ^3. We observe that the system can approach different periodic states depending on initial conditions [20]. The solutions in Figs. 2(a) and 2(b) are obtained for the initial functions $z_0(s) = 0.01(1 + i)\cos(\omega_{\mathrm{in}} s/\tau)$ $(-\tau \leq s \leq 0)$, with $\omega_{\mathrm{in}} = 0.6$ and $\omega_{\mathrm{in}} = 1.6$, respectively. The figure shows that the asymptotic solutions have different frequencies as well. This demonstrates the coexistence of periodic attractors with different frequencies.

In order to find out which coexistent periodic attractors are available in our system, we perform a numerical integration with different frequencies ω_{in} of the initial conditions. The results are shown in Fig. 3 for two different values of delay $\tau = 80$ and $\tau = 500$. The frequencies ω_a of the asymptotic states are plotted versus ω_{in}. We observe that about ten different frequencies appear for $\tau = 80$, which can be realized depending on initial conditions. For $\tau = 500$, this frequency discretization still persists but is no longer visible due to the small distance between the neighboring frequencies.

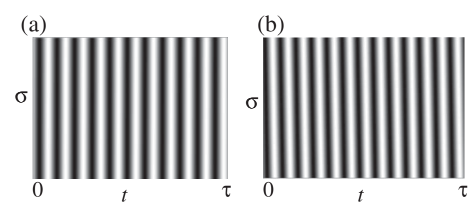

FIG. 2. "Space-time" representation of the asymptotic states of system (1) for $\alpha = -0.8$ shows numerically the coexistence of stable solutions with different frequencies. The real part of z is plotted. The horizontal axis represents the spacelike direction ranging from 0 to τ. Solutions in (a) and (b) have a different number of maxima per delay interval. They are obtained by choosing different initial conditions (see details in the text). $\tau = 80$, $\beta = 1$.

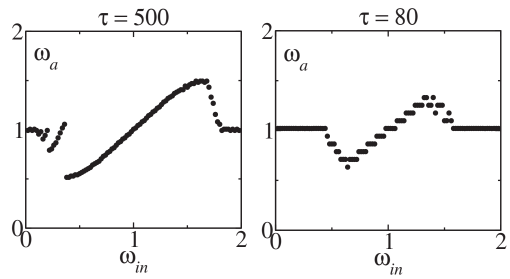

FIG. 3. Frequency of the limiting periodic attractor ω_a as a function of the frequency of the initial condition $\omega_{\rm in}$. Initial condition: $z_0(s) = 0.01(1+i)\cos(\omega_{\rm in} s)$. $\alpha = -0.2$, $\beta = 1$.

Note that Fig. 3 is obtained for a fixed value of the bifurcation parameter $\alpha = -0.2$. Changing α, the range of available frequencies ω_a is varying as well. This dependence of ω_a on α is summarized in Fig. 4, where α varies from the bifurcation point $\alpha = -1$ up to $\alpha = 1$. We observe that the range of available frequencies of periodic attractors ω_a first increases quadratically as α is increased from -1 and then shrinks to the single frequency $\omega_a \approx \beta$ for $\alpha > 0$. Figure 4 shows how the dynamics of the system changes as it goes through the bifurcation. We are now going to describe analytically some important features of this destabilization process. In particular, the analytical arguments in the following section confirm the genericity of the observed phenomenon as well as provide a good quantitative description of the involved dynamical regimes.

Eckhaus instability and amplitude equations.—The phenomena, which are discovered numerically in Figs. 2–4, can be partially understood by using the correspondence between delayed systems and spatially extended systems [19]. In fact, for α close to -1, we observe the Eckhaus instability scenario for a delay system. In order to show this, let us first derive the amplitude equation for (1), which describes the dynamics of the amplitude of destabilized oscillations close to the bifurcation. We assume $\alpha = -1 + \mu\varepsilon^2$, where μ is a new parameter describing small deviations from this bifurcation. Hence, we have

$$z' = (-1 + \mu\varepsilon^2 + i\beta)z + z_\tau - z|z|^2. \tag{4}$$

The procedure of deriving an amplitude equations for the delay system (4) uses a standard multiscale slow-amplitude ansatz: $z(t) = \varepsilon e^{i\beta T_0}[u(\bar{T}) + \varepsilon v(\bar{T}) + \varepsilon^2 w(\bar{T})]$, $\bar{T} = (\varepsilon t, \varepsilon^2 t, \varepsilon^3 t)$ in Eq. (4). A similar technique was used in Refs. [6,19,21]. Therefore, we omit technical details of the derivation, which will be published elsewhere. As a result, we obtain the following Ginzburg-Landau equation:

$$\partial_T \xi = \tfrac{1}{2}\partial^2_{xx}\xi + \partial_x \xi + \mu\xi - \xi|\xi|^2, \tag{5}$$

with the boundary condition $\xi(x, T) = e^{i\varphi}\xi(x-1, T)$. Here $\varphi = -\beta\tau \mod 2\pi$ is the phase change within the delay interval. Given a solution $\xi(x, T)$ of (5), the solution $z(t)$ of the delay system (4) is

$$z(t) = \varepsilon e^{i\beta t}\xi(\varepsilon t - \varepsilon^2 t, \varepsilon^3 t), \tag{6}$$

which is expected to be accurate for a time interval of order ε^{-3}. Note that the linear convection term in (5) can be eliminated by a suitable change of variables. Thus, we obtain

$$\partial_T \xi = \tfrac{1}{2}\partial^2_{xx}\xi + \mu\xi - \xi|\xi|^2. \tag{7}$$

The obtained GL system (7) shows the Eckhaus instability at the bifurcation point $\mu = 0$ (cf. [12]). This phenomenon was first reported in Ref. [11] and it is well known for spatially extended systems [12–15]. We remind the reader that in Eq. (7) it is characterized by the loss of stability of the trivial solution to a periodic pattern of the form $e^{i\beta_c x}$ with the wave number β_c. For systems on an unbounded domain, the trivial state becomes unstable to all periodic patterns e^{iqx}, whose wave number satisfies $(q-\beta_c)^2 \le 2\mu$. However, these periodic solutions are themselves unstable, unless q belongs to the smaller interval $(q-\beta_c)^2 \le \frac{2}{3}\mu$ [22]. The Eckhaus region is the parabolic region in the (q, μ) plane containing stable plane waves. This region is bounded by the Eckhaus parabola

$$\mu_E(q) = \tfrac{3}{2}(q-\beta_c)^2. \tag{8}$$

It has been shown in Ref. [12] that a similar Eckhaus scenario occurs for systems in a large but bounded domain. The main qualitative differences are as follows: (i) The set of allowed frequencies is discretized due to the restrictions imposed by the boundary conditions. (ii) The Eckhaus parabola is shifted downwards

$$\mu_E = \tfrac{3}{2}(q-\beta_c)^2 - \tfrac{1}{4}. \tag{9}$$

We refer to the more detailed analysis of the Eckhaus phenomenon for Eq. (7) in a finite domain to Ref. [12].

Note that, in the theory of amplitude equations for spatially extended systems, Eq. (7) describes the dynamics of the complex amplitude of the pattern via, e.g.,

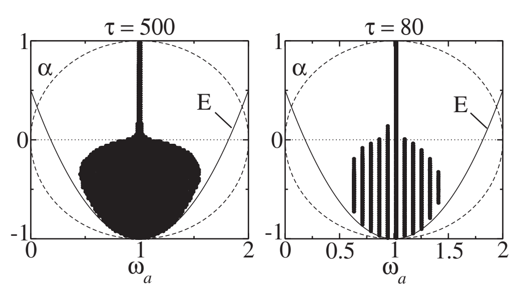

FIG. 4. Dependence of the frequencies of the asymptotic states ω_a on the bifurcation parameter α. Close to the destabilization point at $\alpha = -1$, the system exhibits typical Eckhaus instability. The Eckhaus parabola (E) delineates the stability boundary for the periodic states. For $\alpha > 0$, the zero state is strongly unstable with respect to the single mode with frequency $\beta = 1$ as in the usual Hopf scenario, where no splitting of frequencies occurs.

$w(x, T) = \xi(x, T)e^{i\beta_c x} + \xi^*(x, T)e^{-i\beta_c x}$, while for the delay system we have the relationship (6).

Coming back to our delay system (4), we recall the correspondence between the bifurcation parameters $\varepsilon^2\mu = \alpha + 1$ and the frequencies $\omega_a - \beta = \varepsilon(q - \beta_c)$. Using these scalings, we obtain the Eckhaus parabola for the delay system as

$$\alpha_E + 1 = \frac{3}{2}(\omega_a - \beta)^2 - \frac{\varepsilon^2}{4} \approx \frac{3}{2}(\omega_a - \beta)^2. \qquad (10)$$

We emphasize the following interesting feature: Due to the scaling restrains, our final formula for the Eckhaus region for the delay system (10) is, in fact, approximated by the corresponding formula for the unbounded domain (8) in spite of the fact that the amplitude dynamics is governed by the system on a finite domain.

The Eckhaus curve $\alpha_E(\omega_a)$ is plotted in Fig. 4 (the line with label E). One can note that there is perfect matching of the theoretically predicted results from the amplitude GL model (7) and the numerically obtained results for the delay Eq. (1) in the region, which is close to the bifurcation point $\alpha \approx -1$.

When spatiotemporal representation fails.—The validity of the amplitude Eq. (7) relies on the fact that the curve of the pseudocontinuous spectrum (3) is well approximated by a parabola. This clearly breaks down at $\alpha \approx 0$. Here the local dynamics in the vicinity of the zero state is dominated by the single strongly unstable mode with the eigenvalue $\lambda_S \approx \alpha + i\beta$. This appears to be true even in the presence of the unstable pseudocontinuous spectrum for $\alpha < 1$, and we observe the typical scenario of a Hopf bifurcation with a single periodic attractor.

Summary.—We have studied the destabilization scenario of a system with an oscillatory instability and a long delayed feedback. We have shown that the destabilization occurs in two stages: (i) On the first stage, the Eckhaus phenomenon occurs and multiple coexisting periodic attractors appear. This stage can be nicely approximated by the complex GL equation (5) as an amplitude equation. (ii) On the second stage, the domain with multiple periodic attractors shrinks and one attractor with frequency close to β survives; see Fig. 4. This stage can no longer be explained by the amplitude equations. Instead, a low-dimensional approximation should be used.

Our numerical and analytical studies were done for the simplest specific equation, which includes an oscillatory instability and a long delayed feedback and, hence, is able to display these phenomena. Using the distinction between strong and weak instabilities of delay equations with large delay, we were able to specify the conditions which allow to check easily whether this scenario occurs in any specific model. In particular, it can be verified that the splitting of the single emission mode of a laser with long delayed feedback into so-called external cavity modes can be understood within this context.

Finally, we remark that systems with large delay exhibit many interesting phenomena, which are usually accompanied by a high degree of multistability [23–25]. We show in this Letter that such a multistability is an inherent feature of large-delay systems, since it generically occurs already at the basic oscillatory destabilization bifurcation. The analytical calculations confirm that, as delay increases, the number of such coexisting stable attractors grows linearly.

*Electronic address: wolfrum@wias-berlin.de
†Electronic address: yanchuk@wias-berlin.de

[1] *Theoretical Ecology*, edited by R. M. May (Blackwell Scientific Publishers, Oxford, 1976).
[2] M. C. Mackey and L. Glass, Science **197**, 287 (1977).
[3] M. Schanz and A. Pelster, Phys. Rev. E **67**, 056205 (2003).
[4] W. Wischert, A. Wunderlin, A. Pelster, M. Olivier, and J. Groslambert, Phys. Rev. E **49**, 203 (1994).
[5] J. D. Farmer, Physica (Amsterdam) **4D**, 366 (1982).
[6] G. Giacomelli and A. Politi, Physica (Amsterdam) **117D**, 26 (1998).
[7] T. Heil, I. Fischer, W. Elsäßer, J. Mulet, and C. R. Mirasso, Phys. Rev. Lett. **86**, 795 (2001).
[8] C. E. Carr, Annu. Rev. Neurosci. **16**, 223 (1993).
[9] S. A. Kashchenko, Comput. Math. Math. Phys. **38**, 443 (1998).
[10] P. Hövel and E. Schöll, Phys. Rev. E **72**, 046203 (2005).
[11] W. Eckhaus, *Studies in Non-linear Stability Theory*, Springer Tracts in Natural Philosophy (Springer, New York, 1965).
[12] L. S. Tuckerman and D. Barkley, Physica (Amsterdam) **46D**, 57 (1990).
[13] K. Tsiveriotis and R. A. Brown, Phys. Rev. Lett. **63**, 2048 (1989).
[14] L. Tuckerman and D. Barkley, Phys. Rev. Lett. **67**, 1051 (1991).
[15] N. Mukolobwiez, A. Chiffaudel, and F. Daviaud, Phys. Rev. Lett. **80**, 4661 (1998).
[16] R. Hoyle, *Pattern Formation: An Introduction to Methods* (Cambridge University Press, Cambridge, England, 2006).
[17] S. Yanchuk and M. Wolfrum, in *Proceedings of the Fifth EUROMECH Nonlinear Dynamics Conference (ENOC-2005), Eindhoven, Netherlands, 2005* (Eindhoven University of Technology, Eindhoven, 2005).
[18] S. Lepri, G. Giacomelli, A. Politi, and F. T. Arecchi, Physica (Amsterdam) **70D**, 235 (1994).
[19] G. Giacomelli and A. Politi, Phys. Rev. Lett. **76**, 2686 (1996).
[20] The transient should be of order τ^3. This rule will be confirmed by the amplitude equations, since the scale of the slow time for the amplitude variable is $\varepsilon^3 t$.
[21] M. Nizette, Physica (Amsterdam) **183D**, 220 (2003).
[22] Given formulas for the Eckhaus region differ from the formulas in Ref. [12] by a factor of 2, since we do not rescale the coefficient $1/2$ at ξ_{xx}.
[23] J. Losson, M. C. Mackey, and A. Longtin, Chaos **3**, 167 (1993).
[24] S. Yanchuk, Phys. Rev. E **72**, 036205 (2005).
[25] H.-J. Wünsche *et al.*, Phys. Rev. Lett. **94**, 163901 (2005).